

## Numerical Study on Atmospheric Pressure DBD in Helium: Single-breakdown and Multi-breakdown Discharges

This article has been downloaded from IOPscience. Please scroll down to see the full text article.

2011 Plasma Sci. Technol. 13 724

(<http://iopscience.iop.org/1009-0630/13/6/17>)

View [the table of contents for this issue](#), or go to the [journal homepage](#) for more

Download details:

IP Address: 117.32.153.167

The article was downloaded on 06/06/2012 at 02:25

Please note that [terms and conditions apply](#).

# Numerical Study on Atmospheric Pressure DBD in Helium: Single-breakdown and Multi-breakdown Discharges\*

WANG Xiaohua (王小华), YANG Aijun (杨爱军), RONG Mingzhe (荣命哲),  
LIU Dingxing (刘定新)

State Key Laboratory of Electrical Insulation and Power Equipments,  
Xi'an Jiaotong University, Xi'an 710049, China

**Abstract** A 1-D fluid model for homogeneous dielectric barrier discharge (DBD) in helium is presented, aimed at unraveling the spatial-temporal characteristics of two basic discharge regimes: single-breakdown and multi-breakdown discharges. Discharge currents, gap voltages, charge densities, electron temperature and electric field profiles of the two regimes make it clear that these two regimes are qualitatively different. It is found that the multi-breakdown discharge has a more homogeneous flux on dielectrics compared to the single-breakdown discharge.

**Keywords:** fluid model, single-breakdown discharge, multi-breakdown discharge, dielectric barrier discharge

**PACS:** 52.65.Kj

## 1 Introduction

Dielectric barrier discharge (DBD), also known as silent discharge, is characterized by the presence of an insulating layer in contact with the discharge between two planar or cylindrical electrodes [1]. At atmospheric pressure, DBD typically presents three different modes, i.e., filamentary, regularly patterned and homogeneous discharges [1], depending on the gas composition, operating voltage, electrode configuration, and some other operating conditions.

As a high uniformity of plasma is required for many industrial applications, such as surface modification of materials, the homogeneous plasma generated by DBD is of great interest to researchers [2~7]. Depending on the operating conditions, homogeneous atmospheric pressure DBD can present two modes: the glow mode and Townsend mode, as has been proved by experimental and numerical investigation [6~9]. In principle, the Townsend mode is characterized by a very low density of space charge in the discharge gap that the electric field is hardly disturbed, and the electron density peaks near the anode, while the glow mode has a characteristic structure with a positive column, a Faraday dark space and a strong cathode fall [7].

In order to better control this kind of plasmas for various applications, it is essential to understand the nature of the two modes. A different discharge phenomenon with several current peaks in helium was observed experimentally, which was not operated in the Townsend mode due to relatively large current peaks [3,7]. In order to investigate the fundamental characteristics of the multi-breakdown discharge, a numerical simulation is required, which has been proved to be very helpful in investigations of atmospheric pressure

DBD [10,11]. In this study, we present two regimes of DBD: the single-breakdown and multi-breakdown discharges. It is found that the single-breakdown discharge is in the glow mode while the earlier breakdowns in the multi-breakdown discharge are in the glow mode and the later breakdowns are in the Townsend mode. It is also found that the multi-breakdown discharge has a more homogenous flux on a dielectric surface compared to the single-breakdown discharge.

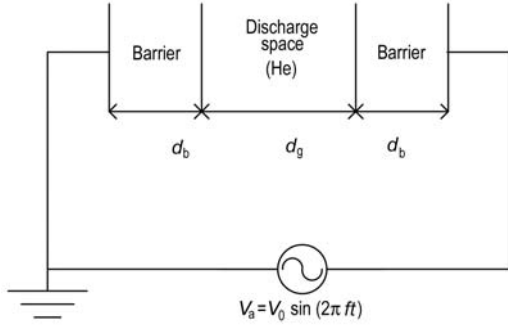
## 2 Description of the model

Fig. 1 shows the schematic diagram of DBD in our model. The plasma is generated between two plane-parallel electrodes covered with an alumina board as a dielectric with a relative dielectric constant  $\epsilon_r=9$ , which is chosen the same way as used by MANGOLINI and co-workers [2]. The dimensions are: the gas gap  $d_g=2$  mm and the alumina board thickness  $d_b=1$  mm, similar to the parameters used by BRANDENBURG and co-workers [12]. A sinusoidal voltage  $V_a = V_0 \sin(2\pi ft)$  is applied to the right electrode and the left electrode is grounded, of which  $f=10$  kHz and  $V_0=1200$  V (single-breakdown discharge) or 2400 V (multi-breakdown discharge). The gas temperature is kept constant at 300 K.

The 1-D numerical model of the homogeneous barrier discharge in helium incorporates five chemical species: electrons ( $e$ ), helium metastable atoms ( $\text{He}^*$ ), helium metastable molecules ( $\text{He}_2^*$ ), singly charged helium positive ions ( $\text{He}^+$ ), helium molecular ions ( $\text{He}_2^+$ ). The electron mobility and diffusivity are calculated as a function of the mean electron energy using a Boltzmann solver [13]. The transport properties of the heavy ions

\*supported by National Natural Science Foundation of China (No. 50907053) and State Key Laboratory of Electrical Insulation and Power Equipment of China (EIPE10305)

and metastables are obtained from literature [14].



**Fig. 1** Schematic diagram of the DBD in 1-D model.  $d_b$ : Barrier thickness,  $d_g$ : Gas gap

The governing equations consist of continuity equations for particle conservation with the drift-diffusion approximation Eq. (1), the electron energy conservation equation Eq. (2) and Poisson equation Eq. (3), as follows:

$$\frac{\partial n_i}{\partial t} + \nabla \cdot \mathbf{\Gamma}_i = S_i, \mathbf{\Gamma}_i = \text{sgn}(q_i) n_i \mu_i \mathbf{E} - D_i \nabla n_i, \quad (1)$$

$$\begin{aligned} & \frac{\partial n_e \varepsilon}{\partial t} + \nabla \cdot \left( \frac{5}{3} \varepsilon \mathbf{\Gamma}_e - \frac{5}{3} n_e D_e \nabla \varepsilon \right) \\ & = -e \mathbf{\Gamma}_e \cdot \mathbf{E} - \sum_j \Delta E_j K_j - 3 \frac{m_e}{m_{\text{He}}} K_{\text{el}} k_b (T_e - T_{\text{He}}), \quad (2) \end{aligned}$$

$$\varepsilon_0 \nabla \cdot \mathbf{E} = \sum_i q_i n_i, \quad (3)$$

where  $n_i$ ,  $\mathbf{\Gamma}_i$ ,  $S_i$ ,  $q_i$ ,  $\mu_i$ ,  $D_i$  represent the density, flux in the drift-diffusion approximation, net creation rate, charge, mobility and diffusion coefficient for species  $i$ ;  $\mathbf{E}$  is the electric field strength;  $\varepsilon$ ,  $e$  are the mean electron energy, and elementary charge;  $E_j$  and  $K_j$  are the energy loss and rate coefficient of reaction  $j$ ;  $m_e$  and  $m_{\text{He}}$  are the masses of electrons and helium;  $K_{\text{el}}$  is momentum transfer rate between electrons and background helium;  $k_b$ ,  $T_e$  and  $T_{\text{He}}$  are the Boltzmann constant, electron temperature, and background helium gas temperature;  $\varepsilon_0$  is vacuum permittivity. The three terms on the right hand side of Eq. (2) represent the electron Joule heating and energy transfer due to inelastic collision and elastic collision.

Boundary conditions at both electrodes and the interface between the gas and dielectric barrier are determined as follows:

**a.** The electron flux to the border is given by the sum of the thermal flux minus the rate of secondary-electron release;

**b.** Secondary-electron emission probability for ion bombardment is set as 0.02;

**c.** The boundary fluxes of metastables ( $\text{He}^*$  and  $\text{He}_2^*$ ) are assumed to be thermally limited;

**d.** The boundary fluxes of heavy ions ( $\text{He}^+$ ,  $\text{He}_2^+$ ) are given by the sum of the mobility and thermal fluxes;

**e.** For simplicity, the electron mean energy at both borders is fixed at 1 eV [11];

**f.** For the Poisson equation, the gas and the barrier interface boundary conditions are given by the surface charge, which is accumulated by conduction current.

The equation system is solved by using a time-dependent solver in COMSOL. The minimum mesh size is 2  $\mu\text{m}$  at the center and 8  $\mu\text{m}$  at the gas-dielectric interface, which gradually expands up to 20  $\mu\text{m}$  at the electrodes.

The reactions and corresponding rate coefficients are listed in Table 1. The rate coefficients  $f(T_e)$  are obtained using the Boltzmann solver [13] and fitted to analytic functions with the mean electron energy as a variable. The other reaction rate coefficients follow the data in literature [9].

**Table 1.** Elementary reactions, the corresponding rates, and the energy loss due to inelastic collision

Reactions	Rate coefficients	$\Delta E$ (eV)
$\text{He} + e = \text{He}^* + e$	$f(T_e)$ [ $\text{cm}^3 \text{s}^{-1}$ ]	19.8
$\text{He} + e = \text{He}^+ + 2e$	$f(T_e)$ [ $\text{cm}^3 \text{s}^{-1}$ ]	24.6
$\text{He}^* + e = \text{He}^+ + 2e$	$f(T_e)$ [ $\text{cm}^3 \text{s}^{-1}$ ]	4.8
$\text{He}_2^+ + e = \text{He}^* + \text{He}$	$8.9 \times 10^{-9} \times (T_e/T_{\text{He}})^{-1.5}$ [ $\text{cm}^3 \text{s}^{-1}$ ]	–
$\text{He}^+ + 2\text{He} = \text{He}_2^+ + \text{He}$	$1.1 \times 10^{-31}$ [ $\text{cm}^6 \text{s}^{-1}$ ]	–
$\text{He}^* + 2\text{He} = \text{He}_2^* + \text{He}$	$2.0 \times 10^{-34}$ [ $\text{cm}^6 \text{s}^{-1}$ ]	–
$2\text{He}^* = \text{He}_2^+ + e$	$1.5 \times 10^{-9}$ [ $\text{cm}^3 \text{s}^{-1}$ ]	–17.2
$\text{He}_2^* + \text{M} = 2\text{He} + \text{M}$	$4 \times 10^4$ [ $\text{s}^{-1}$ ]	–
$2\text{He}_2^* = \text{He}_2^+ + 2\text{He} + e$	$1.5 \times 10^{-9}$ [ $\text{cm}^3 \text{s}^{-1}$ ]	–13.8

## 3 Results and analysis

### 3.1 The single-breakdown discharge regime

As shown in Fig. 2 is the discharge current waveform of single-breakdown discharge in this study. As periodically repeated, the discharge current has one peak per half cycle of the applied voltage. The current pulses have a peak current density of about 22 mA/cm<sup>2</sup>, and a rising time and residual time of about 2  $\mu\text{s}$  and 6  $\mu\text{s}$ , respectively. It is noted that the glow mode is characterized by the narrow current pulse of a large (tens of milliamperes) amplitude and the presence of only one current peak per half cycle [7]. So the single-breakdown discharge in this study should be in the glow mode. In comparison, the filamentary discharge normally has a peak current density of several A/cm<sup>2</sup>, and a lasting time of tens of nanoseconds.

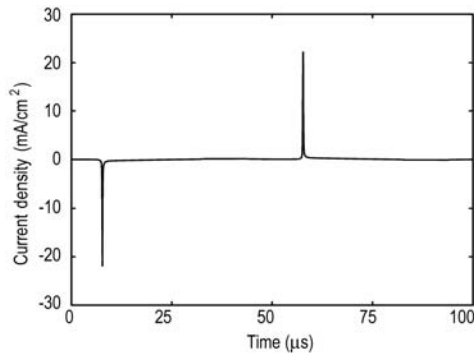


**Fig.2** Discharge current for single-breakdown discharge (The peak amplitude and frequency of applied voltage are 1200 V and 10 kHz respectively)

Fig. 3 shows the temporal profiles of the applied voltage ( $V_a$ ) and gap voltage ( $V_g$ ). At the beginning of each cycle,  $V_g$  increases with  $V_a$  until a discharge happens when  $V_g$  decreases sharply, which is a typical characteristic of the glow discharge. Then the opposite electric field, caused by space charges, stops the discharge quickly and prevents the formation of an arc. After voltage reversing, the deposited charges strengthen the electric field and thus promote the next discharge, so the peak of the discharge current doesn't coincide with that of the applied voltage.

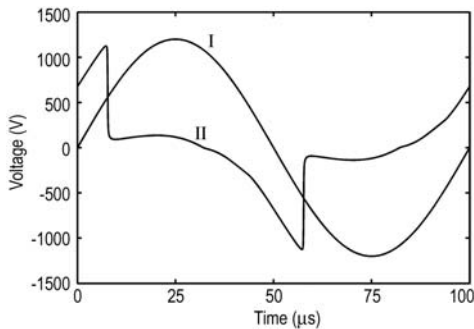


**Fig.3** Applied and gap voltages of single-breakdown discharge:  $V_a$ (I),  $V_g$  (II)

The spatial-temporal profiles of the electron density and temperature are shown in Fig. 4. The electron density has one peak in each half cycle of the applied voltage, which can be reflected by the electron temperature shown in Fig. 4(b). Before the discharge the space charge density is not high enough to disturb the electric field and thus the electron temperature is almost uniform, as shown in Fig. 4(b). With the increase in the applied voltage, the space charge is accumulated and a plasma sheath is formed with a high electric field. In the sheath the electrons are heated, and breakdown happens when the electrons are energetic enough. As the avalanche propagates, the plasma sheath collapses and in consequence the electron temperature decreases sharply. However, the sheath could form again because the operating voltage keeps increasing after breakdown (see Fig. 3). In the sheath region electrons are heated again (see the triangle-shaped tails in Fig. 4(b)). If the applied voltage is high enough, it is possible that a

second breakdown would happen (see Fig. 8, the multi-breakdown discharge). During the discharge the electron loses its energy and thus the electron temperature decreases sharply. After the discharge the electron temperature remains very low and uniform most of the time due to the low space charge density and electric field, as shown in Fig. 4(b).

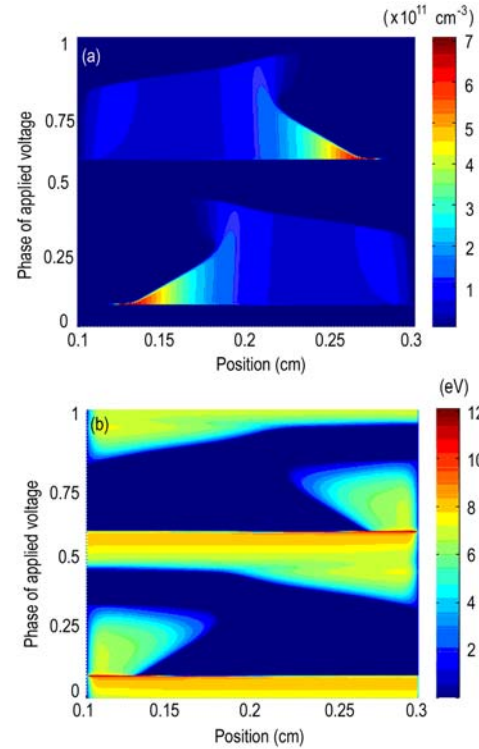


**Fig.4** Spatial-temporal properties of electron density (a) and temperature (b), in single-breakdown discharge

To further confirm the mode of the single-breakdown discharge in this study, we plot in Fig. 5 the spatial distributions of the electrical field strength, ion and electron densities when the current peak is the maximum. Four specific regions can be distinguished: a strong cathode fall, a negative glow, a Faraday dark space and a positive column, which are the most important characteristics of a glow discharge. Therefore, the single-breakdown in this study is definitely in the glow mode.

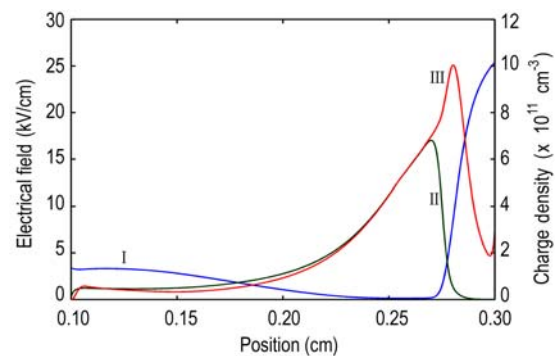


**Fig.5** Calculated electrical field strength (I), electron (II) and ion (III) densities of single breakdown discharge when the current density peak is maximum (Instantaneous anode is on the left)

### 3.2 The multi-breakdown discharge regime

As shown in Fig. 6 is the discharge current waveform of multi-breakdown discharge in this study. As periodically repeated, the discharge current has three peaks per half cycle of the applied voltage. Though multi-breakdown is the phenomenal characteristic of the Townsend mode, the current density peaks are much larger than those of the Townsend mode (no more than  $1 \text{ mA/cm}^2$ ) [7]. So the multi-breakdown can't be simply classified as in the Townsend mode. From the size of current densities, we can predict that Townsend and glow modes co-exist in the multi-breakdown. As can be seen from Fig. 7, the gap voltage increases with the applied voltage until the discharge occurs. It oscillates with the avalanche breakdown, due to the space charge accumulation in each breakdown. Compared to the voltages in single-breakdown discharge shown in Fig. 3, the applied voltage is much higher but the peaks of the gap voltage are comparatively lower. In the multi-breakdown, the magnitudes of current peaks decrease monotonically and the corresponding breakdown voltages have the same trend.

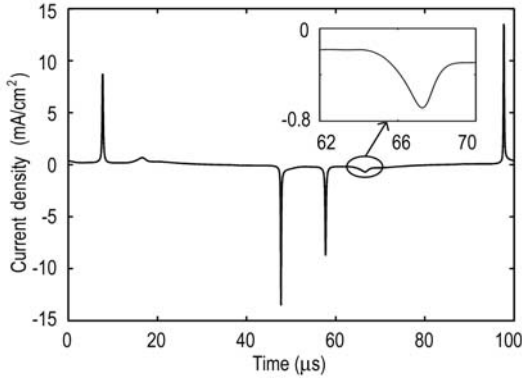


**Fig.6** Discharge current of multi-breakdown discharge (The peak and frequency of applied voltage are 2400 V and 10 kHz respectively)

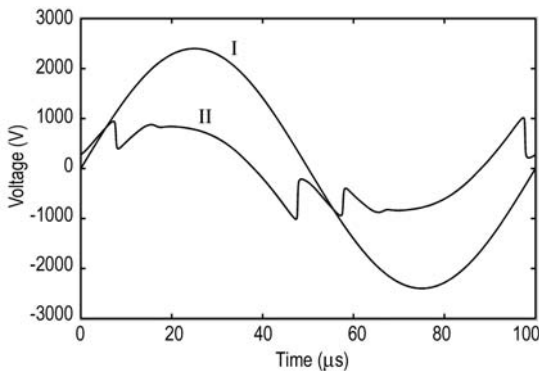


**Fig.7** Applied and gap voltages of multi-breakdown discharge:  $V_a$  (I),  $V_g$  (II)

Compared to the single-breakdown (Fig. 4), the electron has a lower peak density but a comparable peak temperature, as shown in Fig. 8. The electron density has two peaks per half cycle, corresponding to the

first two larger current peaks in Fig. 6. It is noted that the third breakdown is so weak that the electron density peak is very small; therefore, there are only two peaks per half cycle that can be seen in Fig. 8(a). As shown in Fig. 8(b), the electron temperature characteristics in the first two breakdowns are similar to those in Fig. 4(b). However the electron temperature in the third breakdown is always very high but not high enough to cause a glow discharge, because the space charge (mainly positive ions) has a high density all over the space and no sheath is formed. It is also due to the space charge density that a plasma sheath with a very high electric field can be formed several times per half cycle, and thus the breakdown can happen several times.

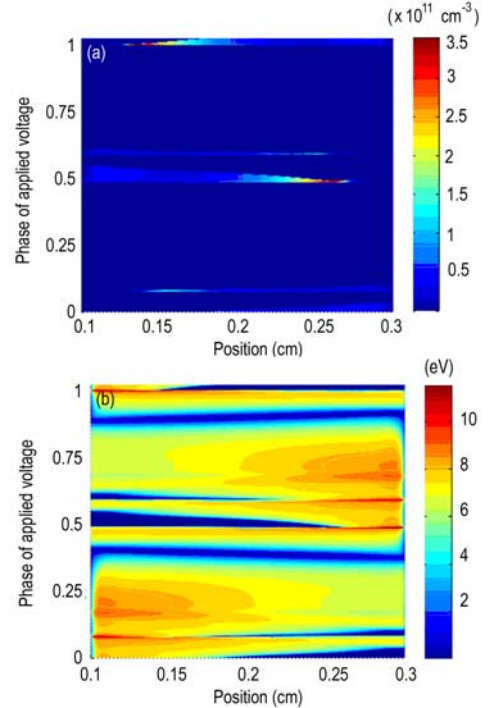


**Fig.8** Spatial-temporal properties of electron density (a), and temperature (b) in multi-breakdown discharge

In order to confirm the discharge modes of the multi-breakdown, in Fig. 9, we plot the spatial distributions of the electrical field strength, ion and electron densities at three moments of  $t_1$ ,  $t_2$ , and  $t_3$  ( $t_1$ ,  $t_2$ , and  $t_3$  are the three moments when the three current peaks have the maximum, respectively). As are shown in Fig. 9(a and b), the characteristics are similar to those in Fig. 5. So the first two breakdowns can be defined as glow discharge. It appears from Fig. 9(c) that the maximum in the electron density is located near the anode and has the maximum of  $10^9 \text{ cm}^{-3}$ , which is indeed typical of a Townsend discharge. Besides, the charge densities are so low that they are not enough to localize the electric field, which refers to another characteristic of the Townsend mode, i.e., the electric field is high and uniform. So the third breakdown can be defined in the Townsend mode. These confirm our prediction that Townsend and glow modes can co-exist in a multi-breakdown, i.e., the earlier breakdowns are more likely

in the glow mode and the later breakdowns are more likely in the Townsend mode. The later discharge can not evolve into a glow discharge due to the eigen field caused by the space charge.

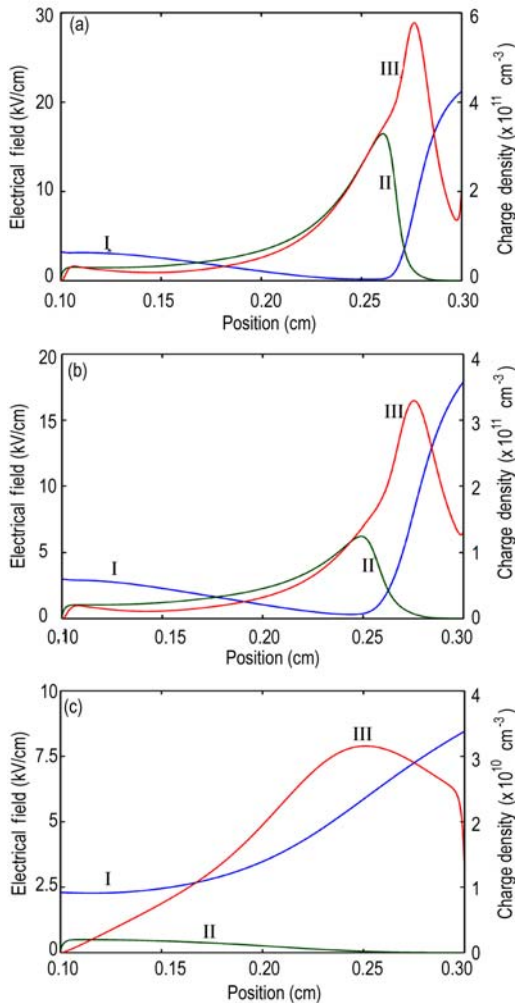


**Fig.9** Calculated field strength (I), electron (II) and ion (III) densities of multi-breakdown discharge at three moments of  $t_1$ (a),  $t_2$ (b), and  $t_3$ (c) (Instantaneous anode is on the left)

Fig. 10 compares the fluxes of electrons, ions and helium metastables on the dielectric surfaces, with respect to the two discharge regimes: single-breakdown discharge (upper) and multi-breakdown discharge (lower). From a point of view of the plasma application, fluxes are sometimes crucial, for in direct plasma treatment one or two dielectric layers could be the sample. The flux of charged species (electrons and ions) dominates the total flux, indicating that charged species should be most responsible for surface treatment in helium plasmas. This is totally inverse to the oxygen-containing plasmas, in which oxygen neutral species are considered to play a dominant role [15]. The fluxes of species have similar profiles to their densities in half an operating voltage cycle, i.e., only one peak in the single-breakdown discharge but several peaks in the multi-breakdown discharge. The flux of helium metastables

has peak shapes due to  $\text{He}^*$ , which has high potential energy (19.8 eV) and is hence sensitive to energetic electrons that exist in the neighborhood of the dielectric layers (sheath).  $\text{He}_2^*$  is comparatively stable, as a consequence the flux of metastables changes only by two orders of magnitude over an operating voltage cycle, much less than that of the charged species. This indicates, for plasma surface treatment, the effect of metastables is much more homogeneous than that of the charged species, especially the ions.

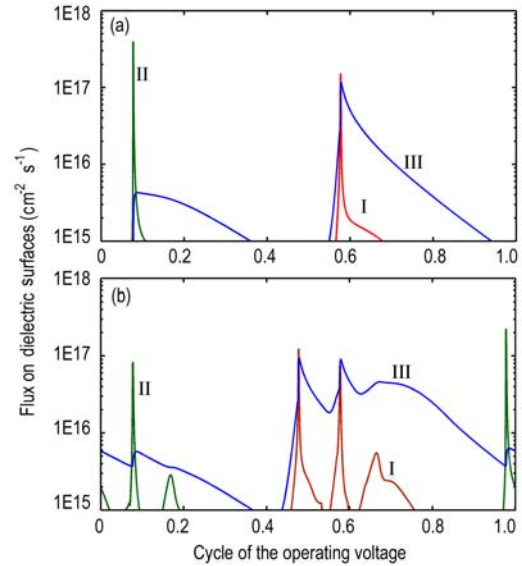


**Fig.10** Flux of different species (I: electron, II: ion, III: helium metastables  $\times 100$ ) on the dielectric surfaces of the two discharge modes: single breakdown (a) and multi-breakdown (b)

Though the discharge intensity in multi-breakdown is weaker than that in single-breakdown, the multi-breakdown discharge has almost the same charged species flux peak as the single-breakdown discharge. In addition, if one looks at the electron profiles carefully, one can find that in the multi-breakdown mode the variation of the electron flux is comparatively high. Therefore, it can be concluded that in the multi-breakdown discharge the fluxes have higher uniformity with a high enough value, and from this viewpoint a multi-breakdown discharge is better for plasma surface treatment.

### 3.3 Conclusion

The spatial-temporal characteristics of the single-breakdown and multi-breakdown discharges of DBD in helium are discussed by means of a 1-D fluid model. Compared to the single-breakdown discharge, the multi-breakdown discharge needs a higher applied voltage, but its electron density, current and gap voltage are comparatively low. In the multi-breakdown, the earlier breakdowns appear to be more in the glow mode while the later breakdowns more in the Townsend mode. It is found that the multi-breakdown discharge

has a more homogeneous effect compared to the single-breakdown discharge in plasma surface treatment.

## References

- 1 Kogelschatz U. 2002, IEEE Trans. on Plasma Science, 30: 1400
- 2 Mangolini L, Anderson C, Heberlein J, et al. 2004, J. Phys. D: Appl. Phys., 37: 1021
- 3 Radu I, Bartnikas R, Wertheimer M R. 2003, IEEE Trans. Plasma Sci., 31: 1363
- 4 Luo Haiyun , Liang Zhuo, Lv Bo, et al. 2007, Appl. Phys. Lett., 91: 221504
- 5 Massines F, Segur P, Gherardi N, et al. 2003, Surface and Coatings Technology, 174~175: 8
- 6 Massines F, Gherardi N, Naude N, et al. 2005, Plasma Phys. Control. Fusion, 47: B577
- 7 Golubovskii Yu B, Maiorov V A, Behnke J, et al. 2003, J. Phys. D: Appl. Phys., 36: 39
- 8 Danijela D. Sijacic, Ute Ebert. 2002, Phys. Rev. E, 66: 066410
- 9 Mangolini L, Orlov K, Kortshagen U, et al. 2002, Appl. Phys. Lett., 80: 1722
- 10 Shi J J, Kong M G. 2007, Appl. Phys. Lett., 90: 111502
- 11 Radu I, Bartnikas R, Wertheimer M R. 2003, J. Phys. D: Appl. Phys., 37: 449
- 12 Brandenburg R, Navrátil Z, Jánský J, et al. 2009, J. Phys. D: Appl. Phys., 42: 085208
- 13 Hagelaar G J M, Pitchford L C. 2005, Plasma Sources Sci. Technol., 14: 722
- 14 Ellis H W, Pai R Y, McDaniel E W, et al. 1976, At. Data Nucl. Data Tables, 17: 177
- 15 Liu D X, Bruggeman P, Iza F, et al. 2010, Plasma Sources Sci. Technol., 19: 025018

(Manuscript received 21 July 2011)

(Manuscript accepted 28 October 2011)

E-mail address of corresponding author LIU Dingxin:

liudingxin@mail.xjtu.edu.cn